https://doi.org/10.5194/acp-2020-1197
Preprint. Discussion started: 29 December 2020

Atmospheric Chemistry and Physics Discussions

Modeling the Impact of COVID-19 on Air Quality in Southern California: Implications for Future Control Policies

Zhe Jiang[1†], Hongrong Shi[1*†], Bin Zhao[2*], Yu Gu[3], Yifang Zhu[4], Kazuyuki Miyazaki[5], Yuqiang Zhang[6], Kevin W. Bowman[3,5], Takashi Sekiya[7], Kuo-Nan Liou[3]

[1] Key Laboratory of Middle Atmosphere and Global Environment Observation, Institute of Atmospheric Physics, Chinese Academy of Sciences, Beijing, China
[2] Pacific Northwest National Laboratory, Richland, WA, USA
[3] Joint Institute for Regional Earth System Science and Engineering and Department of Atmospheric and Oceanic Sciences, University of California, Los Angeles, CA, USA
[4] Institute of Environment and Sustainability, University of California, Los Angeles, CA, USA
[5] Jet Propulsion Laboratory, California Institute of Technology, Pasadena, CA, USA
[6] Nicholas School of the Environment, Duke University, Durham, NC, USA
[7] Japan Agency for Marine-Earth Science and Technology, Yokohama, Japan

Correspon*dence to*: Hongrong Shi (shihrong@mail.iap.ac.cn) and Bin Zhao (bin.zhao@pnnl.gov)

† Zhe Jiang and Hongrong Shi contributed equally to this paper.

Abstract. In response to the Coronavirus Disease 2019 (COVID-19), California issued statewide stay-at-home orders, bringing about abrupt and dramatic reductions in air pollutant emissions. This crisis offers us an unprecedented opportunity to evaluate the effectiveness of emission reductions on air quality. Here we use the Weather Research and Forecasting model with Chemistry (WRF-Chem) in combination with surface observations to study the impact of the COVID-19 lockdown measures on air quality in southern California. Based on activity level statistics and satellite observations, we estimate the sectoral emission changes during the lockdown. Due to the reduced emissions, the population-weighted concentrations of fine particulate matter ($PM_{2.5}$) decrease by 15% in southern California. The emission reductions contribute 68% of the $PM_{2.5}$ concentration decrease before and after the lockdown, while meteorology variations contribute the remaining 32%. Among all chemical compositions, the $PM_{2.5}$ concentration decrease due to emission reductions is dominated by nitrate and primary components. For O_3 concentrations, the emission reductions cause a decrease in rural areas but an increase in urban areas; the increase can be offset by a 70% emission reduction in anthropogenic volatile organic compounds (VOC). These findings suggest that a strengthened control on primary $PM_{2.5}$ emissions and a well-balanced control on nitrogen oxides and VOC emissions are needed to effectively and sustainably alleviate $PM_{2.5}$ and O_3 pollution in southern California.

https://doi.org/10.5194/acp-2020-1197
Preprint. Discussion started: 29 December 2020

Atmospheric Chemistry and Physics Discussions

1 Introduction

Anthropogenic emissions from various emission sources, including transportation, industrial, agricultural, residential, and commercial sectors, contribute to California's long-existing air pollution problems (e.g., Shirmohammadi et al., 2016; Hong et al., 2015; Warneke et al., 2013). The major pollutants include, but are not limited to, fine particulate matter ($PM_{2.5}$), nitrogen dioxide (NO_2), sulfur dioxide (SO_2) and ozone (O_3). Exposure to these pollutants has been correlated with an increased rate of morbidity and mortality (Wang et al., 2019). Mitigating the adverse effects of air pollution by reducing air pollutant emissions from major sectors has been and will continue to be a major public policy challenge. However, the effect of emission reductions from various sources on air quality improvement is subject to substantial uncertainties, because such effect cannot be directly measured and because the atmospheric chemistry processes are highly nonlinear and complicated (Zhao et al., 2019b; Zhao et al., 2015; Chen et al., 2013). The recent Coronavirus Disease 2019 (COVID-19) pandemic provides an unprecedented opportunity for a more robust understanding of the environmental impacts brought by the emission reductions.

More than 200 countries and territories around the world have reported a total of about 53 million confirmed cases of the coronavirus COVID-19 that originated from Wuhan, China, and a death toll of more than 1300K (World Health Organization, 2020). California is one of the most affected states in the United States (U.S.) partly because its poor air quality makes Californians more susceptible to infectious diseases such as COVID-19 (Bashir et al., 2020; Chiara Copat, 2020). In response to the emergence of COVID-19, statewide stay-at-home orders and related actions (e.g., closure of nonessential businesses) took effect on March 19, 2020 in California. These orders are expected to reduce vehicle traffic and industrial activities, thereby changing the air pollutant emissions and air quality in the state. It is essential to obtain a high-spatiotemporal-resolution estimation of air pollution for better understanding of the atmospheric impacts caused by changes in anthropogenic activity associated with the COVID-19 pandemic.

A number of studies emerged soon after the start of the COVID-19 pandemic and the subsequent lockdown to assess the impact of the pandemic on air quality over various regions around the world. For example, Archer et al. (2020) compared the observed concentrations at all available ground monitoring sites in U.S. between April of 2020 and the prior five years (2015–2019) and found statistically significant decreases in NO_2 concentrations at more than 65% of the monitoring sites, with an average drop of 2 ppb. Pan et al. (2020) compared the surface air quality monitoring data in California during the period 20 March–5 May in 2020 with those in 2015–2019 and found that the $PM_{2.5}$ in 2020 exhibited a notable decrease which could result from emission reductions associated with the COVID-19 lockdown. Similar findings, i.e., reduced $PM_{2.5}$ and NO_2 concentrations are also reported for China (e.g., Chu et al., 2020; Le et al., 2020; Liu et al., 2020; Marlier et al., 2020; Shi and Brasseur, 2020; Miyazaki et al., 2020b), India (e.g., Pathakoti et al., 2020; Sharma et al., 2020), and Europe (e.g., Chen et al., 2020; Menut et al., 2020; Sicard et al., 2020; Ordóñez et al., 2020) based on surface and/or satellite observations. For O_3, the concentrations either increased or slightly decreased during the pandemic, depending on regions (Bekbulat et al., 2020; Huang et al., 2020; Pan et al., 2020; Zhao et al., 2020). Most of the above studies, however, are

https://doi.org/10.5194/acp-2020-1197
Preprint. Discussion started: 29 December 2020


Atmospheric Chemistry and Physics Discussions

limited to comparing observations with and without lockdown measures, which correspond to different time periods under different meteorological conditions.

Meteorology plays significant roles in air pollution formation, transport, deposition and transformation (Wang et al., 2020a), which is a very important factor that affects concentrations of O_3 and $PM_{2.5}$ (Stewart et al., 2017). The changes in air quality due to meteorological variations may obscure the effects of emission changes during the COVID-19 lockdown. Using the Community Multi-scale Air Quality model, Wang et al. (2020a) showed that the benefits of emission reductions were overwhelmed by adverse meteorology over the North China Plain and severe air pollution events were thus not avoided. Goldberg et al. (2020) reported that meteorological patterns were especially favorable for low NO_2 in much of the United States in spring 2020, complicating comparisons with spring 2019; the meteorological variations between years can cause ~15% difference in monthly mean column NO_2. In view of this, modelling approach is necessary to accurately assess the impact of lockdown measures by excluding the possible effects of meteorological conditions and to examine the possible mechanisms responsible for the changes in the air pollutant concentrations. In addition, while previous studies have evaluated the air quality changes in different regions due to the emission reductions associated with the COVID-19 lockdown, it remains unclear how the COVID-19 induced emission reductions and the concurrent meteorological variations influence air quality in California.

The objective of this study is to investigate the air quality impact of the emission reductions in southern California in association with COVID-19 by employing high-resolution atmospheric modelling in combination with surface observations. Based on the statistics of activity levels together with constraints from satellite observations, we estimate the sectoral emission changes during the COVID-19 lockdown. We then conduct model simulations using the Weather Research and Forecasting model with Chemistry (WRF-Chem) for the periods before and during the COVID-19 lockdown to investigate the effects of reduced emissions and meteorology on air pollution, respectively. Understanding how air quality responds to the emission reductions during COVID-19 pandemic will provide important insight into the future development and optimization of effective air pollution control strategies in southern California.

2 Method and Data

2.1 Model configuration and emission estimation

We simulate the impact of COVID-19 lockdown measures on air quality using the WRF-Chem version 3.9.1, which considers highly nonlinear and complex meteorological and atmospheric chemistry processes. The simulation period is February 18 to April 23, 2020, which includes about one month before and after the California governor issues the stay-at-home (lockdown) order on March 19 (Pan et al., 2020). We apply the model to two nested domains: Domain 1 covers the western United States and its surrounding areas at a 12 km×12 km horizontal resolution; Domain 2 covers California with a 4 km×4 km resolution (Fig. S1). We focus our analysis on southern California (the red rectangle in Fig. S1), the largest metropolitan area in California which is significantly affected by the lockdown measures. We employ an extended Carbon

https://doi.org/10.5194/acp-2020-1197
Preprint. Discussion started: 29 December 2020

Atmospheric Chemistry and Physics Discussions

Bond 2005 (CB05) (Yarwood et al., 2005) with chlorine chemistry (Sarwar et al., 2008) coupled with the Modal for Aerosol Dynamics in Europe/Volatility Basis Set (MADE/VBS) (Wang et al., 2015a; Ahmadov et al., 2012). MADE/VBS uses a modal aerosol size representation and an advanced secondary organic aerosol (SOA) module based on the VBS approach. The aqueous-phase chemistry is based on the AQChem module used in the Community Multiscale Air Quality (CMAQ) model (Wang et al., 2015a). The chemical initial and boundary conditions were extracted from the output of the Whole Atmosphere Community Climate Model (WACCM) (Marsh et al., 2013). A 6-day spin-up period is used to minimize the influence of initial conditions on simulation results. The vertical resolution, meteorological initial and boundary conditions, and physical options are the same as our previous modeling studies based on WRF-Chem for California (Zhao et al., 2019a; Wang et al., 2020b; Shi et al., 2019).

We obtain anthropogenic emissions in California without the influence of COVID-19 lockdown measures from the California Air Resources Board (CARB) for 2012 that is the latest year in which the data are available (California Air Resources Board, 2018). We scale the 2012 emissions to the 2020 levels by employing the relative changes for 2012–2018 in California from the "NEI trend report" (US Environmental Protection Agency, 2018a) and assuming that the trends continued during 2018–2020. The anthropogenic emissions outside California are derived from the National Emission Inventory (NEI) (US Environmental Protection Agency, 2018b) in 2011 and are scaled to 2020 following the same method. The biogenic, wind-blown dust, sea-salt, and wildfire emissions are calculated online in WRF-Chem, as detailed in our previous studies (Zhao et al., 2019a; Wang et al., 2020b; Shi et al., 2019).

In our baseline simulation ("Base" scenario in Table S1), we use the above emission inventories. To evaluate the effect of the COVID-19 response actions, we conduct another simulation ("Lockdown" scenario in Table S1) in which the CARB anthropogenic emission inventory after March 19 is adjusted to account for the emission changes due to the COVID-19 lockdown. Because of the lack of detailed emission data which often take years to update, we rely on a number of key activity indicators to estimate the sector-specific relative changes in anthropogenic emissions (as summarized in Table S2), which are subsequently evaluated against satellite-derived emission estimate. For the transportation sector, we use weekly production of gasoline, diesel, and jet fuel in California obtained from the "Weekly Fuels Watch Reports" of the California Energy Commission (California Energy Comission, 2020b) to estimate the emission changes from gasoline vehicles, diesel vehicles, and aircraft. The changes in emissions from the industrial, residential, and commercial sectors are assumed to be proportional to the changes in electricity consumption by the corresponding sector, as summarized in the "Energy Insights Reports" of the California Energy Commission (California Energy Comission, 2020a). The changes in emissions from power plants are estimated as a function of the total electricity demand in California (California Energy Comission, 2020a). Having estimated the emission changes using the preceding bottom-up method, we compare the changes in nitrogen oxides (NO_x) emissions with a top-down satellite-based emission inventory—an extended calculation of the Tropospheric Chemistry Reanalysis version 2 (TCR-2) (Miyazaki et al., 2020a). This data product has been obtained from the assimilation of multiple satellite measurements of ozone, CO, NO_2, HNO_3, and SO_2 from the OMI (Ozone Monitoring Instrument), TROPOMI (TROPOspheric Monitoring Instrument), MLS (Microwave Limb Sounder), and MOPITT (Measurement Of Pollution In

https://doi.org/10.5194/acp-2020-1197
Preprint. Discussion started: 29 December 2020

Atmospheric Chemistry and Physics Discussions

The Troposphere) satellite instruments. The reanalysis calculation for the COVID-19 time period was conducted at 0.56° horizontal resolution using a global chemical transport model MIROC-CHASER (Watanabe et al., 2011) and an ensemble Kalman filter technique that optimizes chemical concentrations of various species and emissions of NO_x, SO_2, and CO. The extended reanalysis data for 2020 have already been used by Miyazaki et al. (2020c) to study air quality response to the Chinese COVID-19 lockdown measures. Here we use the NO_x emission product which has a sufficiently high quality on the spatiotemporal scales of interest for this study. Using this product, we first calculate NO_x emissions in a hypothetical scenario without considering the COVID-19 effect, based on emission trends in prior years (2017–2019), and subsequently quantify the emission changes due to the COVID-19 using the difference between the hypothetical and real-world emissions (see details in Fig. S2). The estimated NO_x reduction ratios induced by the COVID-19 lockdown measures averaged during March 19 to April 23 in southern California are 28.3% and 27.2% based on the bottom-up and top-down methods, respectively, indicating a generally good agreement between these two methods. That said, we acknowledge that, since more detailed data to support a more accurate estimation are not yet available, the estimates of the sector-specific relative changes in emissions inevitably involve some degree of uncertainty, which can be improved in the future work.

2.2 Observational data and model evaluation

We use a series of meteorology and air quality observations to evaluate the model performance and help analyze the influence of the COVID-19 lockdown. For meteorology, we use observational data obtained from the National Climatic Data Center (NCDC), where hourly or 3-hour observations of wind speed at 10 m (WS10), temperature at 2 m (T2), and water vapor mixing ratio at 2 m (Q2) are available for 82 sites distributed southern California (the red rectangle in Fig. S1). We compare the WRF-Chem meteorological simulations with these measurements and apply a number of statistical indices defined in Emery et al. (2001) to quantitatively evaluate the model performance, as summarized in Table S3. In general, the model simulations agree fairly well with surface meteorological observations. The performance statistics for WS10, T2 and Q2 are all within the benchmark ranges proposed by Emery et al. (2001).

For air quality, we achieve hourly observations of $PM_{2.5}$, O_3, NO_2 and SO_2 from CARB (California Air Resources Board, 2020) and use them to evaluate the air quality simulations of WRF-Chem (see the Results and Discussion section). The observational data are available at 42 sites for $PM_{2.5}$, 63 sites for O_3, 48 sites for NO_2, and 12 sites for SO_2, in southern California (the red rectangle in Fig. S1) during the simulation period. We do not evaluate the model performance in simulating the chemical composition of $PM_{2.5}$ because the composition data from major observational networks had not been available by the time we completed the present study. Nevertheless, our previous studies using almost the same model configurations showed a fairly good agreement with $PM_{2.5}$ composition observations during January, April, July, and October, 2012 (Zhao et al., 2019a; Wang et al., 2020b).

https://doi.org/10.5194/acp-2020-1197
Preprint. Discussion started: 29 December 2020

Atmospheric Chemistry and Physics Discussions

3 Results and Discussion

3.1 Evaluation of the simulated results with surface observations

In this study, we simulated the major air pollutants using WRF-Chem under two scenarios, Base and Lockdown (Table S1). To evaluate the model performance with regard to the temporal variations in air pollutants, we compared the simulated concentrations of $PM_{2.5}$, maximum daily 8-h average (MDA8) O_3, NO_2 and SO_2 with observational data from CARB in southern California.

Before the COVID-19 lockdown (February 18 to March 18), results from model simulation under the Base scenario (Pre_{Base}) capture the magnitude and temporal evolution of the four key air pollutants reasonably well, with normalize mean biases (NMBs) of 11.7%, 4.5%, -14.4% and 7.8% for $PM_{2.5}$, MDA8 O_3, NO_2, SO_2, respectively (Fig. 1). During the COVID-19 lockdown period (March 19 to April 23), compared to the simulations for the Base scenario ($Post_{Base}$) which overestimates the surface concentrations with NMBs of 28.1%, 1.6%, 21.4% and 39.2% for $PM_{2.5}$, MDA8 O_3, NO_2, SO_2, respectively, the simulated results using the adjusted emission inventory ($Post_{Lockdown}$) not only agree better with surface observations for all the four air pollutants (with NMBs of 10.6%, 1.0%, -12.6% and -13.1% for $PM_{2.5}$, MDA8 O_3, NO_2, SO_2, respectively), but also show generally closer NMBs to those during the pre-lockdown period (Fig. 1). The improvement in model performance is observed for both urban and rural areas. In the urban areas, the NMB for $PM_{2.5}$ drops from 25.8% under the Base scenario to 3.9% under the Lockdown scenario, getting closer to the NMB of 4.0% during the pre-lockdown period. The corresponding NMB in rural areas drops from 29.7% to 15.1%, also getting closer to 17.8% during the pre-lockdown period (Figs. 1e,g). Regarding MDA8 O_3, although the differences between the Base and Lockdown scenarios are quite small (Fig. 1b), the NMB is slightly improved from -1.5% ($Post_{Base}$) to -0.2% ($Post_{Lockdown}$) in urban areas and from 3.2% to 1.5% in rural areas (Figs. 1f,h).

Subsequently, we evaluated the spatial distributions of simulated $PM_{2.5}$ and MDA8 O_3 concentrations using observational data averaged during the pre-lockdown and lockdown periods in southern California (Fig. S3). The Base scenario can simulate the spatial patterns of $PM_{2.5}$ and MDA8 O_3 reasonably well (Figs. S3a-b and d-e), but it overestimates the observations of $PM_{2.5}$ concentrations during the lockdown period ($Post_{Base}$, Fig. S3b). The simulated distributions of $PM_{2.5}$ concentrations under the Lockdown scenario ($Post_{Lockdown}$) match the observations better than those for the Base scenario ($Post_{Base}$) (Figs. S3b-c); the hot spots occurring over the Los Angeles County become less polluted and more consistent with the surface observations after considering the emission reductions associated with the COVID-19 lockdown (Figs. S3b-c).

3.2 Effects of anthropogenic emission reductions and meteorology conditions on air pollutants

Both observations and simulations in Fig. 1 show significant changes in air pollutant concentrations during the COVID-19 lockdown relative to the pre-lockdown period, resulting from a combination of emission reductions and meteorology variations. Our model simulations allow us to quantify the relative contributions of these two factors. Figures 2a-d illustrate population-weighted concentrations of simulated $PM_{2.5}$ components, MDA8 O_3, NO_2 and SO_2 in southern California under

https://doi.org/10.5194/acp-2020-1197
Preprint. Discussion started: 29 December 2020


Atmospheric Chemistry and Physics Discussions

the Base and Lockdown scenarios. The concentration differences between the two scenarios during the lockdown period ($Post_{Lockdown}$–$Post_{Base}$) represent the effect of anthropogenic emission reductions. The differences between the lockdown and pre-lockdown periods under the Base scenario ($Post_{Base}$ and Pre_{Base}) can be regarded as meteorology related variations. Figures 2e-h and S4 further show the spatial distribution of the concentration changes caused by anthropogenic emission reductions and meteorology variations.

The simulated population-weighted NO_2 concentrations during the lockdown decrease by 4.3 ppb (from 10.7 to 6.4 ppb) relative to the pre-lockdown period, of which the anthropogenic emission reductions and meteorology conditions contribute 2.4 ppb (56%) and 1.9 ppb (44%), respectively (Fig. 2c). The decrease in NO_2 concentrations as a result of the anthropogenic emission reductions (27%) is similar to the reduction ratio in NO_x emission (28%), indicating that the NO_x emission reductions can be almost fully transferred to ambient concentrations. According to our emission estimation, over 80% of the NO_x reductions is attributed to the substantially lowered traffic intensity due to the stay-at-home order. The population-weighted concentrations of SO_2 also show a decreasing trend (Fig. 2d). Compared with NO_2, the decrease in SO_2 concentrations due to emission reductions is smaller (17%), partly because power generators and heavy industry (the main sources of SO_2) are less affected by the COVID-19 lockdown (see Table S2).

Coinciding with the decrease in NO_2 and SO_2, the simulated population-weighted $PM_{2.5}$ concentrations decrease by 1.8 $\mu g/m^3$ from 8.7 $\mu g/m^3$ during the pre-lockdown period (Pre_{Base}) to 6.9 $\mu g/m^3$ during the lockdown period ($Post_{Lockdown}$). The emission reductions contribute 1.2 $\mu g/m^3$ (67%) of the above decrease, which translates into a 15% reduction in population-weighted $PM_{2.5}$ concentrations from the levels without the lockdown (i.e., $Post_{Base}$) (Fig. 2a). The decrease occurs almost everywhere across the domain (Fig. 2e), consistent with the results in the last section that $PM_{2.5}$ concentrations are lowered in both urban and rural areas as a result of the emission reductions (Figs. 1e,g). The concentration decrease is higher in urban areas than in rural areas (Figs.2e and 1e,g), with the most significant decline occurring in urban areas of the Los Angeles County (Fig. 2e). In contrast, the meteorology variations can increase the $PM_{2.5}$ concentrations in some regions (mainly the inland regions) and decrease them in others (mainly the coastal regions) (Fig. 2f). The net effect is to reduce the population-weighted concentration by 0.6 $\mu g/m^3$ since the concentration decrease happens to occur in more densely populated regions (Fig. 2a).

The concentrations of $PM_{2.5}$ are affected by emissions of multiple pollutants through both primary emissions and chemical reactions. To further explore the reasons behind the $PM_{2.5}$ concentration changes, we examine the changes in individual chemical components, as shown in Fig. 2a and Fig. S4. Following the emission changes (from $Post_{Base}$ to $Post_{Lockdown}$), all major $PM_{2.5}$ components experience a concentration decrease almost throughout the domain (Fig. S4), since the emissions of essentially all pollutants are reduced to some extent due to the lockdown measures (Table S2). The population-weighted concentrations of nitrate decrease the most (0.42 $\mu g/m^3$), followed by "Others" (0.32 $\mu g/m^3$, including all other components besides the key components listed here), organic matter (OM, 0.16 $\mu g/m^3$), ammonium (0.15 $\mu g/m^3$), black carbon (BC, 0.10 $\mu g/m^3$), and sulfate (from 0.07 $\mu g/m^3$) (Fig. 2a). The largest decrease in nitrate is tied to the substantial reduction in NO_x emissions, which is further explained by a larger reduction ratio in transportation emissions (by 30–70%) compared with

https://doi.org/10.5194/acp-2020-1197
Preprint. Discussion started: 29 December 2020


Atmospheric Chemistry and Physics Discussions

other emission sources (Table S2). In addition, the decreases in "Others", EC, and primary OM (a fraction of the total OM) are attributable to the reductions in primary $PM_{2.5}$ emissions. The overall decrease in these primary chemical components even exceeds that of nitrate; this clearly indicates an important role of primary $PM_{2.5}$ components in improving $PM_{2.5}$ air quality during the lockdown period, although the primary $PM_{2.5}$ emissions have only been reduced by 15%.

The simulated population-weighted O_3 concentrations increase noticeably from 38 ppb in the pre-lockdown period (Pre_{Base}) to 42 ppb ($Post_{Lockdown}$) during the lockdown, and the effects of meteorological changes (i.e. $Post_{Base}-Pre_{Base}$) play a dominant role in the variation of O_3. The O_3 level is strongly affected by ambient conditions like temperature and solar radiation (Wang et al., 2015b). As the temperature gets warmer and the radiation gets stronger over time, the O_3 concentrations are elevated in most areas during the COVID-19 lockdown, compared to the pre-lockdown period (Fig. 2h). The emission reductions cause an O_3 decrease in rural areas but a slight increase in the urban areas (Fig. 2g and Figs. 1f,h), which is consistent with previous findings (Zhao et al., 2019a; Wang et al., 2020b; Martien et al., 2003; Qin et al., 2004). In urban areas where NO_x emissions are high, a volatile organic compounds (VOC)-limited regime is seen, while in rural areas, a NO_x-limited regime is observed (Martien et al., 2003; Qin et al., 2004). It follows that the decrease in NO_x emissions leads to opposite changes in O_3 concentrations in urban and rural areas. The increase and decrease in different areas largely offset each other, resulting in a negligible change in population-weighted O_3 concentrations (0.07 ppb) (Fig. 2b) and a slight decrease in area-averaged O_3 concentrations over the modelling domain (0.77 ppb) (Fig. 2g). Last but not least, the small sensitivity of O_3 to emission reductions is also partly explained by the fact that 75% of the ambient O_3 concentration is background O_3 (Zhao et al., 2019a; Wang et al., 2020b).

3.3 Effects of anthropogenic NO_x and VOC emission reductions on ozone concentration

Our modelling results showed an increase in O_3 in urban areas due to the emission reductions in association with the lockdown during the COVID-19 pandemic. The O_3 concentrations are most significantly affected by emissions of NO_x and VOC (Stewart et al., 2017). To further explore the drivers of the O_3 changes and potential approaches to effectively reduce O_3 concentrations, we conduct three sensitivity experiments involving NOx and VOC emission perturbations, as summarized in Table S1. Figure 3 illustrates population-weighted concentrations of simulated $PM_{2.5}$ components and MDA8 O_3 after the COVID-19 lockdown under these sensitivity scenarios and the spatial distribution of the differences in MDA8 O_3 between the sensitivity scenarios and the Base scenario. The first sensitivity experiment is the VOC1.0 scenario which is the same as "Lockdown" except that the VOC emissions are kept at the level of the "Base" scenario (Table S1). It is used to evaluate the relative contribution of VOC and NO_x reductions to COVID-19 induced O_3 concentration changes. Without the control of VOC emissions in VOC1.0 (Fig. 3c), the increase in urban O_3 concentration relative to the Base scenario becomes larger than the Lockdown scenario (Fig. 2g). This confirms our analysis in the last section that the NO_x emission control elevates urban O_3 concentrations under the VOC-limited regime and meanwhile indicates that the VOC control is conducive to O_3 decrease. To assess the potential effects of strengthened NO_x and VOC control measures, we conduct two other sensitivity

https://doi.org/10.5194/acp-2020-1197
Preprint. Discussion started: 29 December 2020


Atmospheric Chemistry and Physics Discussions

experiments named NO_x0.3 and VOC0.3, which are the same as "Lockdown" except that the anthropogenic NO_x (for the NO_x0.3 scenario) and VOC (for the VOC0.3 scenario) emissions are further reduced to 30% of those in the "Base" scenario. Figs. 3a,b show that strengthened NO_x control further reduces the population-weighted concentrations of $PM_{2.5}$, while further reduction of anthropogenic VOC helps to decrease the concentration of MDA8 O_3. Differences in O_3 concentration clearly illustrate different spatial distribution patterns for urban and suburb areas (Figs. 3d, e). For the suburbs with high O_3 values, reducing anthropogenic NO_x and VOC is conducive to the decline of O_3. For urban areas, however, strengthened control with anthropogenic NO_x reduced by 70% (NO_x0.3) results in even more O_3 increase in the central urban area (Fig. 3d). Amplified ozone pollution has also been reported by Sicard et al. (2020) based on their observational studies in four Southern European cities and Wuhan, China associated with NO_x reductions in response to COVID-19. To control O_3 concentrations in urban areas, VOC control may be an effective method. We find that a 70% reduction in anthropogenic VOC (VOC0.3 scenario) can offset all the increases in O_3 caused by NO_x reduction during the lockdown (Fig. 3e). Furthermore, Wang et al. (2019) found that 75% of the average O_3 concentration in California was due to distant emissions outside the western United States. Many other studies also revealed that the background O_3 dominates over the contribution from local emissions in the western U.S. (Huang et al., 2015; Oltmans et al., 2008; Fiore et al., 2014; Emery et al., 2012; Zhang et al., 2011). Therefore, cooperating with other regions and countries in emission reductions may be another way to control O_3 in urban areas of the southern California.

4 Conclusion and policy implications

In this study, we investigated the air quality impact of the emission reductions in southern California in association with COVID-19 by employing WRF-Chem to conduct high-resolution atmospheric modeling during February 18 to April 23, 2020.

Based on the statistics of activity levels, we first adjusted the emission inventory considering the emission reductions during the COVID-19 lockdown. The adjusted emission inventory is shown to be consistent with the emission inventory based on satellite observations. The simulated magnitude and temporal evolution of the concentrations of the key air pollutants, including $PM_{2.5}$, NO_2, SO_2, and MDA8 O_3 using the adjusted emission inventory agree better with surface observations than simulation results without considering the COVID-19 induced emission reductions. Due to the reduced emissions, the population-weighted concentrations of NO_2 and $PM_{2.5}$ decreased by 27% and 15%, respectively, in southern California in the five weeks after the stay-at-home orders. Emission reductions and meteorological variations contributed about two-thirds and one-third, respectively, to the total decrease in population-weighted $PM_{2.5}$ concentrations before and after the lockdown. For O_3 concentration, however, the COVID-19 related emission reductions caused a decrease in suburb areas but a slight increase in the urban areas. In order to further explore the effects of anthropogenic NO_x and VOC emission reductions on O_3 concentration, we conducted sensitivity experiments by strengthening VOC and NO_x controls. Our results showed that strengthened control with NO_x reduced by 70% (NO_x0.3) results in even more O_3 increase in the central urban area and

https://doi.org/10.5194/acp-2020-1197
Preprint. Discussion started: 29 December 2020


Atmospheric Chemistry and Physics Discussions

anthropogenic VOC control may be an effective method to reduce O_3 concentrations in urban areas. A 70% reduction in anthropogenic VOC can effectively offset all the increases in O_3 caused by NO_x reduction during the lockdown.

Using the COVID-19 as an unprecedented experiment with substantial emission reductions from multiple sectors, especially transportation, this study helps to elucidate the complex and nonlinear response of chemical compositions to air pollution control measures and thus provides important insight into the development and optimization of effective air pollution control strategies in southern California. We find that the reduced NO_x emission (~28%) has been almost fully transferred to the reduction in ambient concentration of NO_2 (~27%). This further translates into a remarkable reduction in nitrate, which makes the largest contribution to $PM_{2.5}$ concentration decrease among all individual chemical components. Therefore, to alleviate the $PM_{2.5}$ pollution, measures focusing on sectors such as transportation, which is among the main sources of NO_x emission, could be effective. Moreover, we find that a moderate 15% reduction of primary $PM_{2.5}$ emissions has resulted in a substantial reduction in ambient $PM_{2.5}$ concentrations, with the total concentration decreases in all primary $PM_{2.5}$ components exceeding that of nitrate. Therefore, a strengthened control on primary $PM_{2.5}$ emissions could be an effective strategy to sustainably mitigate $PM_{2.5}$ pollution. For O_3, reduction of NO_x can effectively reduce the high O_3 concentrations in suburban areas, but may cause an increase of urban concentrations. A 70% VOC emission reduction is found to fully offset the urban O_3 increase caused by the lockdown. Therefore, the reduction in NO_x emissions needs to be accompanied by a well-balanced reduction in VOC emissions to avoid the side effect on urban O_3 pollution.

Data Availability Statement

The data from the California Air Resources Board (CARB) monitoring stations used in the present study can be obtained from https://www.arb.ca.gov/aqmis2/aqdselect.php. The meteorology observational data obtained from the National Climatic Data Center (NCDC) can be freely downloaded from ftp://ftp.ncdc.noaa.gov/pub/data/noaa/. Other data needed to support the findings of this study are in the manuscript and the Supplementary Information.

Acknowledgments

B.Z. was partially supported by the DOE Atmospheric System Research (ASR) programme. Y.G. and K.N.L. acknowledge the support by the NSF AGS-1660587, NASA TASNNP program, and NOAA-DOE CPT program. Y.G. and Y.Z. acknowledge the support by the LADWP Award# 20200288. Part of this work was conducted at the Jet Propulsion Laboratory, California Institute of Technology, under contract with NASA. K.M. and K.B. acknowledge the support by the NASA Atmospheric Composition: Aura Science Team Program (19-AURAST19-0044). We would like to acknowledge

https://doi.org/10.5194/acp-2020-1197
Preprint. Discussion started: 29 December 2020

Atmospheric Chemistry and Physics Discussions

high-performance computing support from Cheyenne (https://doi.org/10.5065/D6RX99HX) provided by NCAR's Computational and Information Systems Laboratory, sponsored by the National Science Foundation. We also acknowledge the use of data products from the NASA Aura and EOS Terra and Aqua satellite missions from https://earthdata.nasa.gov. We also acknowledge the free use of the tropospheric NO_2 column data from the SCIAMACHY, GOME-2, and OMI sensors from http://www.qa4ecv.eu and from TROPOMI.

References

Ahmadov, R., McKeen, S. A., Robinson, A. L., Bahreini, R., Middlebrook, A. M., de Gouw, J. A., Meagher, J., Hsie, E. Y., Edgerton, E., Shaw, S., and Trainer, M.: A volatility basis set model for summertime secondary organic aerosols over the eastern United States in 2006, J Geophys Res-Atmos, 117, D06301, DOI 10.1029/2011jd016831, 2012.

Archer, C. L., Cervone, G., Golbazi, M., Fahel, N. A., and Hultquist, C.: Changes in air quality and human mobility in the US during the COVID-19 pandemic, arXiv preprint arXiv:2006.15279, 2020.

Bashir, M. F., Bilal, B. M., and Komal, B.: Correlation between environmental pollution indicators and COVID-19 pandemic: A brief study in Californian context, Environmental Research, 109652, 2020.

Bekbulat, B., Apte, J. S., Millet, D. B., Robinson, A., Wells, K. C., and Marshall, J. D.: PM2. 5 and Ozone Air Pollution Levels Have Not Dropped Consistently Across the US Following Societal Covid Response, 2020.

California Air Resources Board, Air Quality Data: https://www.arb.ca.gov/aqmis2/aqdselect.php, access: May 19, 2020.

CEPAM: Emission Projections By Summary Category: https://www.arb.ca.gov/app/emsinv/fcemssumcat/fcemssumcat2016.php, access: October 1, 2018, 2018.

Energy Insights: https://www.energy.ca.gov/data-reports/energy-insights, access: July 1, 2020, 2020a.

Weekly Fuels Watch Report: https://ww2.energy.ca.gov/almanac/petroleum_data/fuels_watch/index_cms.html, access: July 1, 2020, 2020b.

Chen, D., Li, Q., Stutz, J., Mao, Y., Zhang, L., Pikelnaya, O., Tsai, J. Y., Haman, C., Lefer, B., and Rappenglück, B.: WRF-Chem simulation of NOx and O3 in the LA basin during CalNex-2010, Atmospheric Environment, 81, 421-432, 2013.

Chen, L.-W. A., Chien, L.-C., Li, Y., and Lin, G.: Nonuniform impacts of COVID-19 lockdown on air quality over the United States, Science of The Total Environment, 141105, 2020.

Chiara Copat, A. C., Maria Fiora, Alfina Grasso, Pietro Zuccarello, Salvatore Santo Signorelli, Gea Oliveri Conti, Margherita Ferrante: The role of air pollution (PM and NO2) in COVID-19 spread and lethality: a systematic review, 191, https://doi.org/10.1016/j.envres.2020.110129, 2020.

Chu, B., Zhang, S., Liu, J., Ma, Q., and He, H.: Significant concurrent decrease in PM2. 5 and NO2 concentrations in China during COVID-19 epidemic, Journal of Environmental Sciences, 2020.

Emery, C., Tai, E., and Yarwood, G.: Enhanced meteorological modeling and performance evaluation for two texas episodes. Report to the Texas Natural Resources Conservation Commission, ENVIRON International Corporation, Novato, CA, 2001.

Emery, C., Jung, J., Downey, N., Johnson, J., Jimenez, M., Yarvvood, G., and Morris, R.: Regional and global modeling estimates of policy relevant background ozone over the United States, Atmospheric Environment, 47, 206-217, 10.1016/j.atmosenv.2011.11.012, 2012.

Fiore, A. M., Oberman, J. T., Lin, M. Y., Zhang, L., Clifton, O. E., Jacob, D. J., Naik, V., Horowitz, L. W., Pinto, J. P., and Milly, G. P.: Estimating North American background ozone in U.S. surface air with two independent global models: Variability, uncertainties, and recommendations, Atmospheric Environment, 96, 284-300, 10.1016/j.atmosenv.2014.07.045, 2014.

Goldberg, D. L., Anenberg, S. C., Griffin, D., McLinden, C. A., Lu, Z., and Streets, D. G.: Disentangling the impact of the COVID‐19 lockdowns on urban NO2 from natural variability, Geophysical Research Letters, e2020GL089269, 2020.

Hong, A., Schweitzer, L., Yang, W., and Marr, L. C.: Impact of temporary freeway closure on regional air quality: a lesson

https://doi.org/10.5194/acp-2020-1197
Preprint. Discussion started: 29 December 2020

Atmospheric Chemistry and Physics Discussions

from Carmageddon in Los Angeles, United States, Environmental Science & Technology, 49, 3211-3218, 2015.

Huang, M., Bowman, K. W., Carmichael, G. R., Lee, M., Chai, T. F., Spak, S. N., Henze, D. K., Darmenov, A. S., and da Silva, A. M.: Improved western US background ozone estimates via constraining nonlocal and local source contributions using Aura TES and OMI observations, J Geophys Res-Atmos, 120, 3572-3592, 10.1002/2014jd022993, 2015.

Huang, X., Ding, A., Gao, J., Zheng, B., Zhou, D., Qi, X., Tang, R., Wang, J., Ren, C., and Nie, W.: Enhanced secondary pollution offset reduction of primary emissions during COVID-19 lockdown in China, National Science Review, 2020.

Le, T., Wang, Y., Liu, L., Yang, J., Yung, Y. L., Li, G., and Seinfeld, J. H.: Unexpected air pollution with marked emission reductions during the COVID-19 outbreak in China, Science, 369, 702-706, 2020.

Liu, F., Page, A., Strode, S. A., Yoshida, Y., Choi, S., Zheng, B., Lamsal, L. N., Li, C., Krotkov, N. A., and Eskes, H.: Abrupt decline in tropospheric nitrogen dioxide over China after the outbreak of COVID-19, Science Advances, eabc2992, 2020.

Marlier, M. E., Xing, J., Zhu, Y., and Wang, S.: Impacts of COVID-19 response actions on air quality in China, Environmental Research Communications, 2, 075003, 10.1088/2515-7620/aba425, 2020.

Marsh, D. R., Mills, M. J., Kinnison, D. E., Lamarque, J. F., Calvo, N., and Polvani, L. M.: Climate Change from 1850 to 2005 Simulated in CESM1(WACCM), J Climate, 26, 7372-7391, 10.1175/jcli-d-12-00558.1, 2013.

Martien, P. T., Harley, R. A., Milford, J. B., and Russell, A. G.: Evaluation of incremental reactivity and its uncertainty in southern California, Environmental science & technology, 37, 1598-1608, 2003.

Menut, L., Bessagnet, B., Siour, G., Mailler, S., Pennel, R., and Cholakian, A.: Impact of lockdown measures to combat Covid-19 on air quality over western Europe, Science of The Total Environment, 741, 140426, 2020.

Miyazaki, K., Bowman, K., Sekiya, T., Eskes, H., Boersma, F., Worden, H., Livesey, N., Payne, V. H., Sudo, K., Kanaya, Y., Takigawa, M., and Ogochi, K.: An updated tropospheric chemistry reanalysis and emission estimates, TCR-2, for 2005–2018, Earth System Science Data Discussions, DOI 10.5194/essd-2020-30, 2020a.

Miyazaki, K., Bowman, K., Sekiya, T., Jiang, Z., Chen, X., Eskes, H., Ru, M., Zhang, Y., and Shindell, D.: Air Quality Response in China Linked to the 2019 Novel Coronavirus (COVID‐19) Lockdown, Geophysical research letters, 47, e2020GL089252, 2020b.

Miyazaki, K., Bowman, K. W., Sekiya, T., Jiang, Z., Chen, X., Eskes, H., Ru, M., Zhang, Y., and Shindell, D. T.: Air quality response in China linked to the 2019 novel Coronavirus (COVID-19) mitigation, Geophys Res Lett, 2020c.

Oltmans, S. J., Lefohn, A. S., Harris, J. M., and Shadwick, D. S.: Background ozone levels of air entering the west coast of the US and assessment of longer-term changes, Atmospheric Environment, 42, 6020-6038, 10.1016/j.atmosenv.2008.03.034, 2008.

Ordóñez, C., Garrido-Perez, J. M., and García-Herrera, R.: Early spring near-surface ozone in Europe during the COVID-19 shutdown: Meteorological effects outweigh emission changes, Science of The Total Environment, 141322, 2020.

WHO Coronavirus Disease (COVID-19) Dashboard: https://www.who.int/emergencies/diseases/novel-coronavirus-2019/situation-reports/, access: November 13, 2020, 2020.

Pan, S., Jung, J., Li, Z., Hou, X., Roy, A., Choi, Y., and Gao, H. O.: Air Quality Implications of COVID-19 in California, Sustainability, 12, 7067, 2020.

Pathakoti, M., Muppalla, A., Hazra, S., Dangeti, M., Shekhar, R., Jella, S., Mullapudi, S. S., Andugulapati, P., and Vijayasundaram, U.: An assessment of the impact of a nation-wide lockdown on air pollution–a remote sensing perspective over India, Atmospheric Chemistry and Physics Discussions, 1-16, 2020.

Qin, Y., Tonnesen, G., and Wang, Z.: One-hour and eight-hour average ozone in the California South Coast air quality management district: trends in peak values and sensitivity to precursors, Atmospheric Environment, 38, 2197-2207, 2004.

Sarwar, G., Luecken, D., Yarwood, G., Whitten, G. Z., and Carter, W. P. L.: Impact of an updated carbon bond mechanism on predictions from the CMAQ modeling system: Preliminary assessment, J Appl Meteorol Clim, 47, 3-14, 10.1175/2007jamc1393.1, 2008.

Sharma, S., Zhang, M., Gao, J., Zhang, H., and Kota, S. H.: Effect of restricted emissions during COVID-19 on air quality in India, Science of the Total Environment, 728, 138878, 2020.

Shi, H. R., Jiang, Z., Zhao, B., Li, Z. J., Chen, Y., Gu, Y., Jiang, J. H., Lee, M., Liou, K. N., Neu, J. L., Payne, V. H., Su, H., Wang, Y., Witek, M., and Worden, J.: Modeling Study of the Air Quality Impact of Record-Breaking Southern California Wildfires in December 2017, J Geophys Res-Atmos, 124, 6554-6570, 10.1029/2019jd030472, 2019.

Shi, X., and Brasseur, G. P.: The Response in Air Quality to the Reduction of Chinese Economic Activities during the COVID‐19 Outbreak, Geophysical Research Letters, e2020GL088070, 2020.

https://doi.org/10.5194/acp-2020-1197
Preprint. Discussion started: 29 December 2020

Shirmohammadi, F., Hasheminassab, S., Saffari, A., Schauer, J. J., Delfino, R. J., and Sioutas, C.: Fine and ultrafine particulate organic carbon in the Los Angeles basin: Trends in sources and composition, Science of The Total Environment, 541, 1083-1096, 2016.

Sicard, P., De Marco, A., Agathokleous, E., Feng, Z., Xu, X., Paoletti, E., Rodriguez, J. J. D., and Calatayud, V.: Amplified ozone pollution in cities during the COVID-19 lockdown, Science of The Total Environment, 139542, 2020.

Stewart, D. R., Saunders, E., Perea, R. A., Fitzgerald, R., Campbell, D. E., and Stockwell, W. R.: Linking air quality and human health effects models: an application to the Los angeles air basin, Environmental health insights, 11, 1178630217737551, 2017.

Air Pollutant Emissions Trends Data: https://www.epa.gov/air-emissions-inventories/air-pollutant-emissions-trends-data, access: December 10, 2018, 2018a.

National Emissions Inventory (NEI): https://www.epa.gov/air-emissions-inventories/national-emissions-inventory-nei, access: December 10, 2018, 2018b.

WACCM: https://www.acom.ucar.edu/waccm/download.shtml.

Wang, K., Zhang, Y., Yahya, K., Wu, S. Y., and Grell, G.: Implementation and initial application of new chemistry-aerosol options in WRF/Chem for simulating secondary organic aerosols and aerosol indirect effects for regional air quality, Atmos Environ, 115, 716-732, 10.1016/j.atmosenv.2014.12.007, 2015a.

Wang, P., Chen, K., Zhu, S., Wang, P., and Zhang, H.: Severe air pollution events not avoided by reduced anthropogenic activities during COVID-19 outbreak, Resources, Conservation and Recycling, 158, 104814, 2020a.

Wang, T., Zhao, B., Liou, K.-N., Gu, Y., Jiang, Z., Song, K., Su, H., Jerrett, M., and Zhu, Y.: Mortality burdens in California due to air pollution attributable to local and nonlocal emissions, Environment international, 133, 105232, 2019.

Wang, T. Y., Jiang, Z., Zhao, B., Gu, Y., Liou, K. N., Kalandiyur, N., Zhang, D., and Zhu, Y. F.: Health co-benefits of achieving sustainable net-zero greenhouse gas emissions in California, Nature Sustainability, 10.1038/s41893-020-0520-y, 2020b.

Wang, Z., Li, Y., Chen, T., Zhang, D., Sun, F., Wei, Q., Dong, X., Sun, R., Huan, N., and Pan, L.: Ground-level ozone in urban Beijing over a 1-year period: Temporal variations and relationship to atmospheric oxidation, Atmospheric Research, 164, 110-117, 2015b.

Warneke, C., De Gouw, J. A., Edwards, P. M., Holloway, J. S., Gilman, J. B., Kuster, W. C., Graus, M., Atlas, E., Blake, D., and Gentner, D. R.: Photochemical aging of volatile organic compounds in the Los Angeles basin: Weekday - weekend effect, Journal of Geophysical Research: Atmospheres, 118, 5018-5028, 2013.

Watanabe, S., Hajima, T., Sudo, K., Nagashima, T., Takemura, T., Okajima, H., Nozawa, T., Kawase, H., Abe, M., Yokohata, T., Ise, T., Sato, H., Kato, E., Takata, K., Emori, S., and Kawamiya, M.: MIROC-ESM 2010: model description and basic results of CMIP5-20c3m experiments, Geosci Model Dev, 4, 845-872, 10.5194/gmd-4-845-2011, 2011.

Yarwood, G., Rao, S., Yocke, M., and Whitten, G. Z.: Final Report-updates to the Carbon Bond Chemical Mechanism: CB05 (RT-04-00675), Yocke and Co., Novato, California, 246, 2005.

Zhang, L., Jacob, D. J., Downey, N. V., Wood, D. A., Blewitt, D., Carouge, C. C., van Donkelaar, A., Jones, D. B. A., Murray, L. T., and Wang, Y. X.: Improved estimate of the policy-relevant background ozone in the United States using the GEOS-Chem global model with 1/2 degrees x 2/3 degrees horizontal resolution over North America, Atmospheric Environment, 45, 6769-6776, 10.1016/j.atmosenv.2011.07.054, 2011.

Zhao, B., Wang, S., Xing, J., Fu, K., Fu, J., Jang, C., Zhu, Y., Dong, X., Gao, Y., and Wu, W.: Assessing the nonlinear response of fine particles to precursor emissions: development and application of an extended response surface modeling technique v1. 0, Geoscientific Model Development (Online), 8, 115-128, 2015.

Zhao, B., Wan, T. Y., Jiang, Z., Gu, Y., Liou, K. N., Kalandiyur, N., Gao, Y., and Zhu, Y. F.: Air Quality and Health Cobenefits of Different Deep Decarbonization Pathways in California, Environ Sci Technol, 53, 7163-7171, 10.1021/acs.est.9b02385, 2019a.

Zhao, B., Wang, S., Ding, D., Wu, W., Chang, X., Wang, J., Xing, J., Jang, C., Fu, J. S., and Zhu, Y.: Nonlinear relationships between air pollutant emissions and PM2. 5-related health impacts in the Beijing-Tianjin-Hebei region, Science of The Total Environment, 661, 375-385, 2019b.

Zhao, Y., Zhang, K., Xu, X., Shen, H., Zhu, X., Zhang, Y., Hu, Y., and Shen, G.: Substantial Changes in Nitrate Oxide and Ozone after Excluding Meteorological Impacts during the COVID-19 Outbreak in Mainland China, Environmental Science & Technology Letters, 7, 402-408, 2020.

https://doi.org/10.5194/acp-2020-1197
Preprint. Discussion started: 29 December 2020

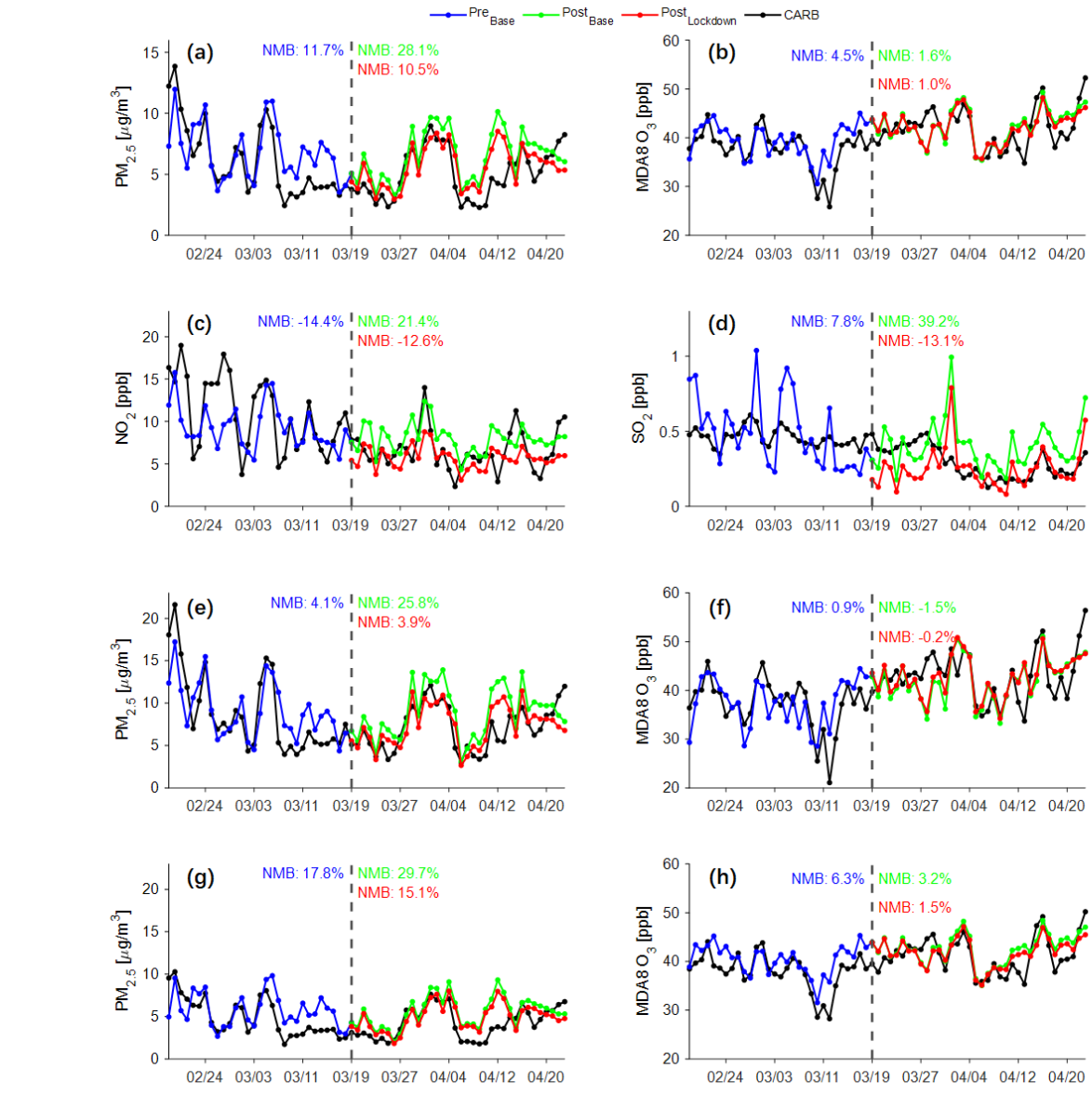

Figure 1: Time series of observed and simulated concentrations of major pollutants. (a-d) Time series of (a) $PM_{2.5}$, (b) MDA8 O_3, (c) NO_2, and (d) SO_2 averaged across all observational stations from CARB over southern California. (e-f) Time series of (e) $PM_{2.5}$ and (f) MDA8 O_3 across all stations over the urban areas of southern California. (g-h) The same as (e-f) but for the rural areas. Black lines are surface observations from the CARB network. Blue, green, and red lines are simulated air pollutant concentrations during the pre-lockdown period (February 18 to March 18) under the Base scenario (Pre_{Base}), during the lockdown period (March 19 to April 23) under the Base scenario ($Post_{Base}$), and during the lockdown period under the Lockdown scenario ($Post_{Lockdown}$). The definitions of the Base and Lockdown scenarios are summarized in Table S1. Normalized mean bias (NMB) is given by $= \sum_{i=1}^{N}(Var_m - Var_o)/\sum_{i=1}^{N} Var_o$, where N is the number of sites, Var_m and Var_o are modeled and observed concentrations, respectively.

https://doi.org/10.5194/acp-2020-1197
Preprint. Discussion started: 29 December 2020

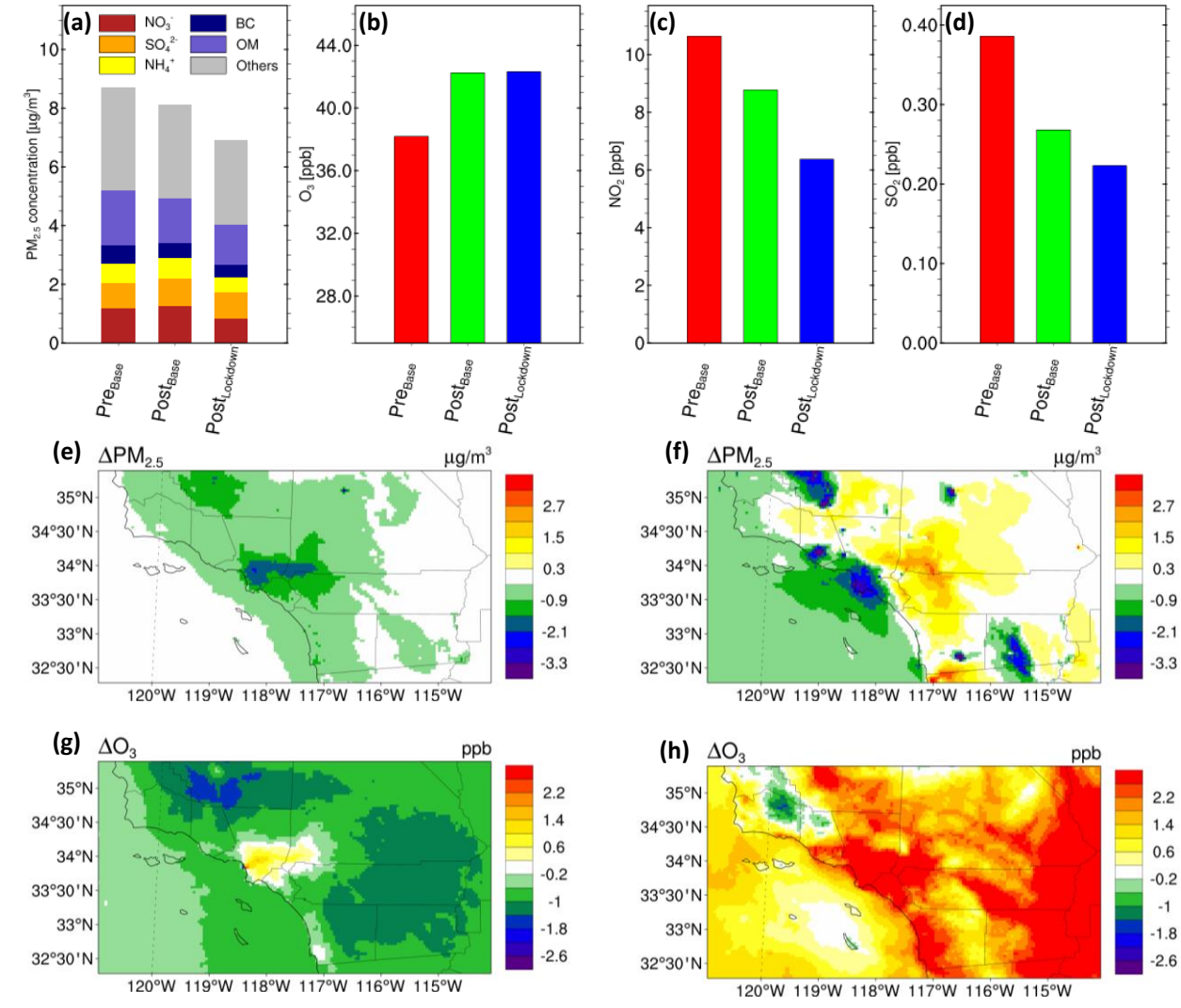

475 **Figure 2: Effects of emission reductions and meteorology conditions on air pollutants. (a-d) Population-weighted concentrations of simulated air pollutant concentrations in southern California: (a) $PM_{2.5}$ components; (b) MDA8 O_3; (c) NO_2; (d) SO_2. Pre_{Base}, $Post_{Base}$, and $Post_{Lockdown}$ have the same meanings as in Fig. 1. (e-h) Spatial distributions of the effects of (e, g) emission reductions and (f, h) meteorology variations on (e, f) $PM_{2.5}$ and (g, h) MDA8 O_3 concentrations.**

https://doi.org/10.5194/acp-2020-1197
Preprint. Discussion started: 29 December 2020

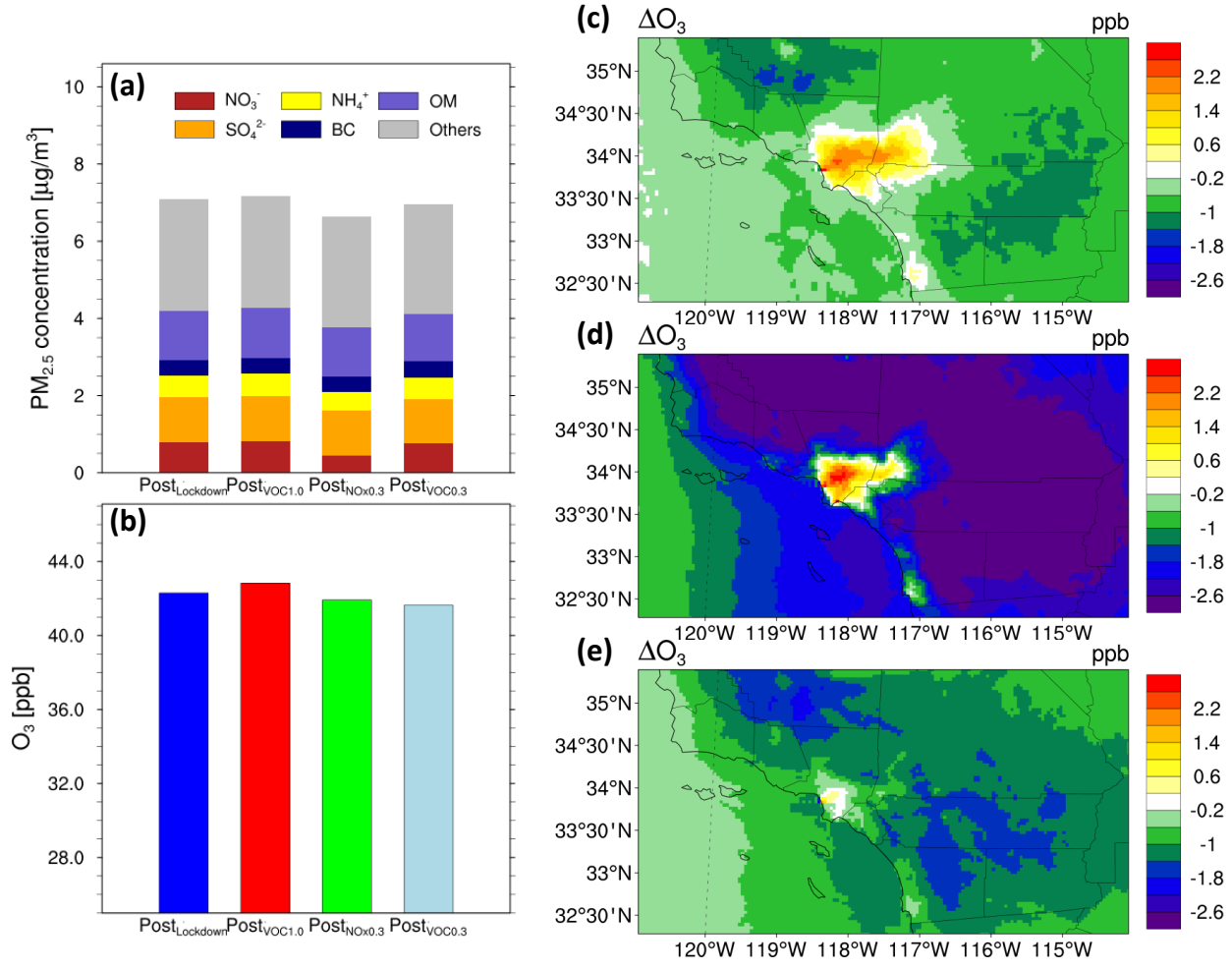

Figure 3: Simulated $PM_{2.5}$ and O_3 concentrations under three sensitivity scenarios during the lockdown period (March 19 to April 23). (a-b) Population-weighted concentrations of (a) $PM_{2.5}$ components and (b) MDA8 O_3 under three sensitivity scenarios (VOC1.0, NO_x0.3 and VOC0.3) and the Lockdown scenario. (c-e) Spatial distribution of the differences in MDA8 O_3 between the three sensitivity scenarios and the Base scenario: (c) VOC1.0 minus Base; (d) NO_x0.3 minus Base; (e) VOC0.3 minus Base. The definitions of all scenarios are summarized in Table S1.